

# Toxicity of different forms of graphene in a chicken embryo model

Maciej Szmidt<sup>1</sup> · Ewa Sawosz<sup>2</sup> · Kaja Urbańska<sup>1</sup> · Sławomir Jaworski<sup>2</sup> ·  
Marta Kutwin<sup>2</sup> · Anna Hotowy<sup>2</sup> · Mateusz Wierzbicki<sup>2</sup> · Marta Grodzik<sup>2</sup> ·  
Ludwika Lipińska<sup>3</sup> · André Chwalibog<sup>4</sup>

Received: 24 October 2015 / Accepted: 4 July 2016 / Published online: 19 July 2016  
© Springer-Verlag Berlin Heidelberg 2016

**Abstract** In the present work, the toxicity of three forms of graphene: pristine graphene (pG), graphene oxide (GO), and reduced graphene oxide (rGO) was investigated using a chicken embryo model. Fertilized chicken eggs were divided into the control group and groups administered with pG, GO, and rGO, in concentrations of 50, 500, and 5000 µg/ml. The experimental solutions were injected in ovo into the eggs, and at day 18 of incubation, the embryo survival, body and organ weights, the ultrastructure of liver samples, and the concentration of 8-hydroxy-2'-deoxyguanosine (8-OHdG) in the livers were measured. Survival of embryos decreased significantly after treatment with all types of graphene, but not in a dose-dependent manner. The body weights were only slightly affected by the highest doses of graphene, while the organ weights were not different among treatment groups. In all experimental groups, atypical hepatocyte ultrastructure and mitochondrial damage were observed. The concentration of the marker of DNA damage 8-OHdG in the liver significantly decreased after pG and rGO treatments. Further in vivo studies with different animal models are necessary to clarify the level of toxicity of different types of graphene and to estimate the

concentrations appropriate to evaluate their biomedical applications and environmental hazard.

**Keywords** Graphene · Graphene oxide · Chicken embryo · Toxicity · Liver · Tem · DNA damage

## Introduction

Nowadays, there is heightened interest and research in the application of the new nanomaterial—graphene. Graphene is a single atomic layer of sp<sup>2</sup>-bonded carbon nanostructure (Geim and Novoselov 2007) that is increasingly considered for multiple medicinal applications as well as for drug delivery systems. The thinnest two-dimensional allotrope of carbon may be considered as a vehicle to deliver drugs to sick cells (Zhang et al. 2012; Chen et al. 2013; Liu et al. 2013). However, the biomedical applications of graphene still have limitations. Graphene toxicity and potential side effects on healthy tissues have been reported (Liao et al. 2011; Bianco 2013; Chang et al. 2011). Recently, a number of studies report different toxic characteristics depending on the form of graphene (reviewed in Chowdhury et al. 2013). However, it is worth noting that most of the investigations were carried out using in vitro models. Thus, the presented work compared the toxicity of different forms of graphene in experiments conducted in vivo, in a chicken embryo model.

Graphene is available for medical research (depending on the method of graphene production) in three main forms: natural or pristine (pG), graphene oxide (GO), and reduced graphene oxide (rGO) (Dreyer et al. 2010). The key difference between these forms is their affinity to water. pG and rGO are recognized as hydrophobic, while GO shows hydrophilic features (Sanchez et al. 2012). All three types of graphene elicit different levels of toxic

---

Responsible editor: Markus Hecker

✉ André Chwalibog  
ach@sund.ku.dk

<sup>1</sup> Department of Morphological Sciences, Warsaw University of Life Sciences, 02-787 Warsaw, Poland

<sup>2</sup> Department of Animal Nutrition and Biotechnology, Warsaw University of Life Sciences, 02-787 Warsaw, Poland

<sup>3</sup> Institute of Electronic Materials Technology, 02-787 Warsaw, Poland

<sup>4</sup> Department of Veterinary Clinical and Animal Sciences, University of Copenhagen, 1870 Frederiksberg, Denmark

effects in experiments conducted *in vitro* as well as *in vivo*, depending on the doses administered (reviewed in Jastrzębska et al. 2012). At 0.4 mg, GO was highly toxic in experiments conducted in mice, and it was not eliminated by the kidneys (Wang et al. 2011). Zhang et al. (2011) compared GO with other carbon nanomaterials and revealed that GO, at a high dose (10 mg/kg), exhibited a long blood circulation time and may lead to pathological changes like pulmonary edema or granuloma formation. Furthermore, GO showed concentration-dependent effects in neurons (Zhang et al. 2010), HeLa cells (Zhang et al. 2012), or erythrocytes (Liao et al. 2011). However, lactate dehydrogenase was released by GO-treated cells independently of their concentration (Zhang et al. 2012). Systematic studies on GO distribution in organisms showed that GO accumulated mainly in the liver and spleen after intraperitoneal injection; however, inflammation and granulomas formation were not observed in treated mice (Yang et al. 2013a, b) when the oral injections of 50 to 100 mg/kg per mouse were applied. Additional studies showed pro-inflammatory characteristics (Wang et al. 2011) with doses 0.1–0.4 mg, pro-autophagy at the concentration of 5 or 100  $\mu\text{g/ml}$  (Chen et al. 2012), or pro-apoptotic activity (10–100  $\mu\text{g/ml}$ ) (Vallabani et al. 2011) characteristics. Other *in vitro* experiments presented cytotoxic features of pG. In studies conducted on macrophages, depletion of the mitochondrial membrane potential, reactive oxygen species production, and apoptosis were detected (Li et al. 2012). It was also demonstrated that GO in concentration 0.1–10 mg/l has different stability in different aqueous environments (Lanphere et al. 2014).

In our previous *in vivo* experiments, 50  $\mu\text{g/ml}$  of pG affected chicken embryo survival; however, it had no impact on the body and investigated organ weights (Sawosz et al. 2014). *In vitro* research suggested that pG and rGO might be less toxic than GO (Zhang et al. 2010; Liao et al. 2011). In terms of biomedical applications, we already demonstrated *in vitro* that pristine graphene can significantly induce mortality of glioblastoma cells at the concentration of 5  $\mu\text{g/ml}$  or higher (Jaworski et al. 2015). We also showed that GO and rGO can affect the viability and proliferation of glioma cells at a concentration of 10  $\mu\text{g/ml}$  and greater (Jaworski et al. 2015). However, to our knowledge, there are no published studies comparing the toxicity of pG, GO, and rGO dose dependently using *in vivo* models.

Recently, it was demonstrated that graphene causes oxidative damage of DNA (Hinzmann et al. 2014; Qiu et al. 2014). Among numerous types of oxidative DNA damage, the formation of 8-hydroxy-2'-deoxyguanosine (8-OHdG) is a marker of oxidative stress and is considered a DNA damage product (Singh et al. 2011). Therefore, to compare the toxicity of different forms of graphene, we investigated its antioxidant

potential on the developing organism by evaluating the concentration of 8-OHdG.

Chicken embryos are a unique well-designed animal model for toxicity evaluations at the level of the functioning organism, due to their sensitivity to the administrated treatments, and isolation from the influence of the external environment (Gagnon and Patel 2007). The early stages of the chick rapid embryonic growth and development are a sensitive model system for investigating the potential toxic effects on body weight, developing organs, and DNA oxidative damage. Therefore, the objective of the study was to evaluate the toxicity of different types of graphene on the growing chicken embryo model taking into account different doses of the evaluated agents.

## Materials and methods

### Nanoparticles

pG powder, produced by liquid-phase exfoliation of graphite, was purchased from Skyspring Nanomaterials (Houston, TX, USA). The purity of the material was >99.5 % with a specific surface area of 120–150  $\text{m}^2 \text{g}^{-1}$ . GO and rGO were obtained from the Institute of Electronic Materials Technology (Warsaw, Poland). GO was prepared by a modified Hummers method from natural graphite flakes (Asbury Carbons). In a synthesis reaction, 5 g of graphite was added into 125 ml of  $\text{H}_2\text{SO}_4$ , and 3.25 g of  $\text{KNO}_3$  was added before the start of the reaction. Subsequently, the beaker with reagents was maintained below 5 °C in a water/ice bath. An amount of 15 g of  $\text{KMnO}_4$  was added in portions into the mixture. After delivering the last portion of oxidant, the beaker was taken out of the bath and kept 1 h at 30–35 °C with continuous stirring and then was left at room temperature for 15 h. In the next step, deionized water was added into the stirred mixture so that the temperature did not exceed 35 °C. The beaker was placed into a water bath at a temperature of 35 °C and stirred for another 1 h. The constantly stirred mixture was then heated to 95 °C and kept under these conditions for 15 min. To stop the reaction, 280 ml of deionized water and 5 ml of  $\text{H}_2\text{O}_2$  were added. The mixture was rinsed with HCl solution to remove sulfate ions and then rinsed with deionized water to remove chloride ions.

The rGO was prepared by chemical reduction of GO. To prepare the reducing mixture, 0.01 g of ammonium iodide, 9 g of hydrated sodium hypophosphite and 1.21 g of sodium sulfite were dissolved in 100 ml of deionized water. The water suspension of 50 mg of GO was acidified to pH = 1 and heated to 90 °C. Then, 12 ml of previously prepared reducing mixture was added. During reduction, the immediate precipitation of a black material (rGO) was observed. The product was filtered, washed with deionized water, and dried.

All graphenes were dispersed in Milli-Q water to prepare experimental suspensions. The flakes were examined using a JEM-2000EX transmission electron microscope (TEM) at 80 keV (JEOL, Tokyo, Japan) with a Morada 11-megapixel camera (Olympus Soft Imaging Solutions GmbH, Münster, Germany). Samples of pG, GO, and rGO suspensions (50 µg/ml) for TEM (Fig. 1) were prepared by placing one droplet of the suspension onto formvar-coated copper grids (Agar Scientific Ltd., Stansted, UK) and dried.

The zeta potential of pG, GO, and rGO suspended in Milli-Q water was measured on a Zetasizer Nano-ZS90 (Malvern Instruments, Worcestershire, UK).

### Animal model

Fertilized eggs ( $55 \pm 2.1$  g) from Ross Line 308 hens, purchased from a commercial hatchery, were stored for 3 days at 10 °C. The eggs were weighed and randomly divided into 11 groups, each with 30 eggs and placed in the incubator under standard conditions. The control group was not treated, the placebo group was injected with phosphate buffered solution, the experimental groups were injected with pG, GO, and rGO, suspended in Milli-Q water, at concentrations of 50, 500, and 5000 µg/ml. 0.3 ml of the experimental suspensions were injected into the egg albumen using 1 ml tuberculin syringes. At day 18 of incubation, the eggs were opened and not fertile eggs were discarded. The fertility in all groups was about 95 %. The alive embryos (cf. Fig. 2) were weighed and decapitated, 1 ml of blood from the jugular vein was collected, and the embryos were examined according to the standard of Hamburger and Hamilton (1952). The liver, heart, brain, and spleen were dissected and weighed. From each group, ten samples of the liver were fixed in liquid nitrogen and stored at -80 °C for pending analyses or were prepared for TEM examination.

Four hours after collection from the jugular vein, blood samples were centrifuged at 3000g for 15 min (Sorvall ST 16, Thermo Fisher Scientific, Waltham, USA) to obtain blood serum. The activity of alanine aminotransaminase (ALT), asparagine aminotransaminase (ASP), and lactate dehydrogenase (LDH) were examined by using the dry chemistry equipment Vitros DT 60 II (Johnston and Johnston, New Brunswick, USA).

### Ultrastructural examination of liver tissue

Liver tissues from all experimental groups were fixed for transmission electron microscopy (TEM) examination in a fixative consisting of 1 % glutaraldehyde in phosphate-buffered saline at pH 7.2. After fixation, the samples were postfixed in 1 % osmium tetroxide and dehydrated in a graded ethanol series. The tissues were embedded in an epoxy embedding resin (Fluka Epoxy Embedding Medium Kit; Sigma-Aldrich). Ultrathin sections (100 nm) were cut with an ultramicrotome (Leica EM UC6, Leica Microsystems Nussloch, Germany) and stained with uranyl acetate and lead citrate. The samples were viewed using a TEM at 80 keV (JEOL, Tokyo, Japan) with a Morada 11 megapixel camera (Olympus Soft Imaging Solutions GmbH, Münster, Germany).

### Evaluation of oxidative DNA damage

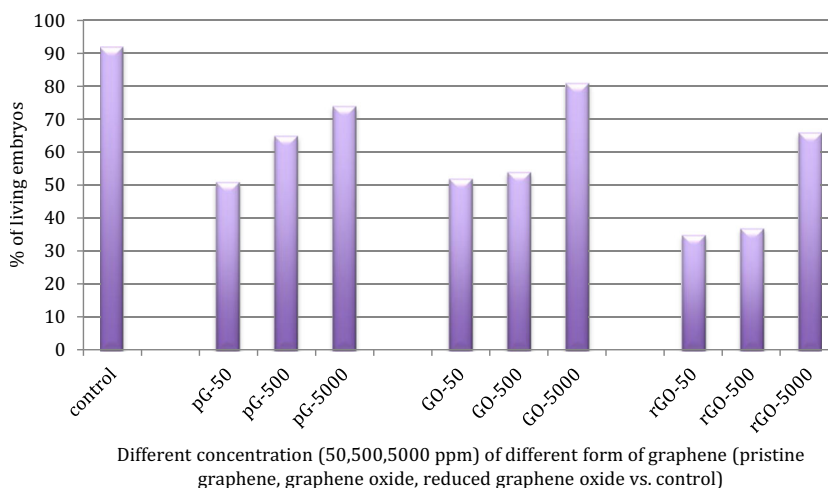
DNA samples were isolated with the FitAmp General Tissue Section Isolation Kit (Epigentek Group Inc., Farmingdale, NY, USA) accordingly to the manufacturer's guide. Samples were lysed in a water bath at 37 °C. DNA was purified on enclosed columns and washed out with elution buffer. Quantification of DNA damage was performed using a colorimetric method. The EpiQuik 8-OHdG DNA Damage Direct Kit (Epigentek Group Inc.) was used to detect the level of 8-OHdG as a marker of oxidative DNA damage, using capture and detection antibodies. The signal was detected and quantified colorimetrically by reading the absorbance in a spectrophotometric microplate reader Infinite M200 (TECAN, Crailsheim, Germany) at a wavelength of 450 nm. All samples were measured in duplicate.

Thiobarbituric acid reactive substances (TBARS) were evaluated according to Fraga et al. (1988). The liver samples were homogenized using TissueLyser LT (Qiagen, Germantown, MD, USA) with a pre-frosted adapter at 50 Hz for 10 min, followed by centrifugation at 13,000×g for 10 min at 4 °C (Sorvall® ST16, Thermo Fisher Scientific). The supernatant ("homogenate") was collected for analysis. Liver homogenates (0.5 ml) were added to 0.5 ml of 3 % sodium dodecyl sulfate and after mixing, 2 ml of 0.1 N HCl, 0.3 ml of 10 % phosphotungstic acid, and 1 ml of 0.7 % 2-thiobarbituric acid



**Fig. 1** TEM images of pristine graphene (a), graphene oxide (b), and reduced graphene oxide (c)

**Fig. 2** The chicken embryo survival at day 18 of incubation. Note: Values for the placebo group (not shown) were similar to the control group



were added. After heating for 30 min in boiling water, TBARS were extracted into 5 ml of l-butanol. After centrifugation, the fluorescence of the butanol layer was measured at 515 nm by spectrometry using an Infinite M200 instrument (TECAN, Crailsheim, Germany).

**Data analysis**

Data were initially checked for normal distribution using the Shapiro-Wilk test. Statistical significance was determined by one-way analysis of variance (ANOVA) using Statgraphics® Plus 4.1 (StatPoint Technologies, Warrenton, VA, USA).  $P \leq 0.05$  was defined as statistically significant.

**Results**

**Characterization of nanoparticles and colloids**

The three forms of graphene differed in the shape and size of the flakes (Table 1). The pG flakes had a surface area ranging from 400 nm to 10 μm, the GO flakes varied from 100 nm to 10 μm, and rGO ranged from 100 nm to 1.5 μm. The zeta potential, which is an indicator of

colloid stability, was the lowest for GO and highest for rGO and pG.

**Growth and development**

The survival rate of embryos decreased after injection of pG, GO, and rGO in all experimental doses compared to the control group (Fig. 2). However, in terms of the mortality, we found inverse correlation between chicken embryo survival and the investigated graphene concentrations. The survival at the 18th day of incubation was the highest for the pG5000, GO5000, and rGO5000 and the lowest for the pG50, GO50, and rGO50. Administration of pG (and also insignificantly rGO at the level of 5000 μg/ml) reduced the body weight of embryos in comparison to the control and other experimental groups (Table 2). The weight of the liver, heart, brain and spleen of embryos at day 18 did not differ significantly between the groups (Table 2). Examination of the chicken embryos according to the Hamburger–Hamilton standard did not reveal any abnormalities in all experimental groups.

Biochemical indices of blood serum were not affected by the treatments (Table 3).

**Table 1** Physical and chemical characterization of pristine graphene (pG), graphene oxide (GO), and reduced graphene oxide (rGO)

Shape	pG Irregular, angular, single to a few layers	GO Film-like, rounded, single layers	rGO Irregular, frayed, a few layers
Average size, μm	1.86	1.27	2.53
Potential zeta, mV <sup>a</sup>	-19.9/-8.7	-49.8/-30.5	-25.1/-9.9
Surface chemical bonds <sup>b</sup>	C=C	C-H, C=C, C=O, C-O, C-H	C=O, C=C, C-O

<sup>a</sup> For the concentration of 50/500 μg/ml

<sup>b</sup> Determined by Fourier transform infrared spectroscopy (Kurantowicz et al. 2015)

**Table 2** Weight of the body and organs of chicken embryos at day 18, after injection of pristine graphene (pG), graphene oxide (GO), and reduced graphene oxide (rGO) at the concentration of 50, 500, and 5000 µg/ml and without injection in the control and with placebo injection

Groups	Concentration, µg/ml	Weight, g				
		Body	Liver	Heart	Brain	Spleen
Control	0	30.6a	0.61	0.25	0.83	0.022
Placebo	50	30.2a	0.59	0.26	0.81	0.023
	500	31.0a	0.62	0.25	0.80	0.022
	5000	30.1a	0.59	0.25	0.82	0.024
Forms of graphene pG	50	29.7a	0.56	0.24	0.83	0.023
	500	27.2ab	0.56	0.22	0.82	0.019
	5000	26.7b	0.56	0.21	0.78	0.021
GO	50	28.0a	0.57	0.25	0.85	0.022
	500	29.6a	0.59	0.25	0.78	0.023
	5000	28.4a	0.57	0.24	0.84	0.018
rGO	50	30.6a	0.61	0.22	0.87	0.022
	500	30.8a	0.64	0.25	0.86	0.027
	5000	27.6ab	0.61	0.23	0.75	0.024
ANOVA						
SEM		2.121	0.088	0.015	0.051	0.001
<i>P</i> value		0.0282	ns	ns	ns	ns

Values with different letters within columns are significantly different  
SEM pooled standard error of means, ns not significant ( $P > 0.05$ )

## Ultrastructural examination of livers

### Control group

In the control group, most nuclei of the examined hepatocytes were euchromatic with visible nucleoli. The heterochromatin was clumped and located mainly peripherally, close to the nuclear membrane (Fig. 3a, b). Glycogen was observed as accumulations of electron-dense particles as well as in large lipid droplets. A large number of mitochondria were noted. Their shapes were round, oval, or elongated. The tubular cristae were short and disarrayed. The tendency of the mitochondria was to localize around the nucleus. Mitochondrial divisions were rarely observed. Abundant rough endoplasmic reticulum closely surrounded the mitochondria.

### After treatment with pG

In the examined samples, disruption of the cell membrane and also a high number of small vesicles were observed. In some cases, the evidence of matrix and cytoplasmic lucency was observed. Mitochondria with interrupted inner and outer membranes and degenerated cristae were visible (Fig. 3e, f). A mitochondrial hyperfusion process was also noted.

**Table 3** The blood serum indices and concentration of 8-OHdG and TBARS in the livers of chicken embryos at day 18, after injection of forms of graphene: pristine graphene (pG), graphene oxide (GO), and reduced graphene oxide (rGO) at the concentration of 50, 500, and 5000 µg/ml and without injection in the control and with injection with placebo

Groups	Concentration, µg/ml	Blood serum indices, U/l			Oxidative status	
		ALT	ASP	LDH	8-OHdG concentration, % DNA	TBARS, ng/100 g tissue
Control	0	19.5	215.3	1089	18.1a	8.1
Placebo	50	21.6	199.0	977	19.2a	9.1
	500	23.1	212.0	1011	18.4a	8.9
	5000	20.5	201.0	1109	19.0a	9.5
Forms of graphene						
pG	50	18.3	201.2	1211	9.7b	9.3
	500	22.1	189.1	1243	11.6b	8.0
	5000	20.9	201.8	1033	17.7a	9.1
GO	50	21.4	183.2	1121	17.1a	10.9
	500	18.9	199.3	1201	15.0ab	9.7
	5000	17.1	184.6	1032	18.1a	10.5
rGO	50	23.1	211.7	1020	10.3b	8.2
	500	19.5	198.5	986	11.2b	7.9
	5000	22.1	213.1	1045	18.5a	9.1
ANOVA						
SEM		1.39	16.22	112.5	1.404	0.674
<i>P</i> value		ns	ns	ns	0.000	ns

Values with different letters within columns are significantly different  
SEM pooled standard error of means, ns not significant ( $P > 0.05$ )

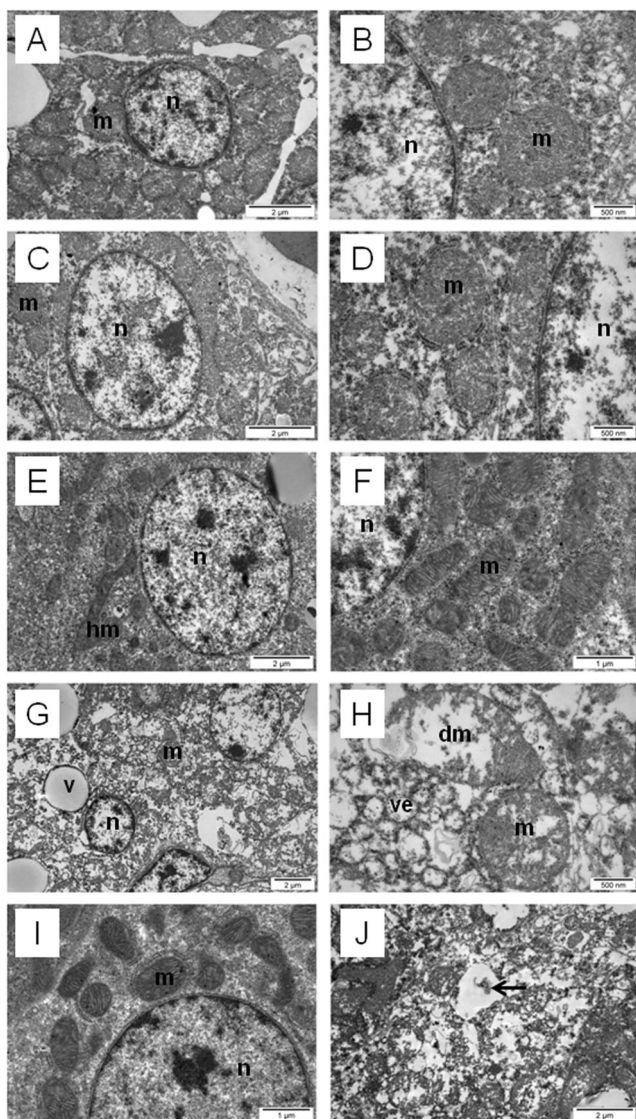


**Fig. 3** TEM images of liver ultrastructure. **a, b** Control group. **c, d** Placebo group. **e, f** Reduced graphene oxide group. **g, h** Pristine graphene group. **i, j** Graphene oxide group. *N* nucleus, *m* mitochondria, *hm* hyperfused mitochondria, *dm* damaged mitochondria, *ve* vesicle; *arrow* indicates graphene oxide nanoparticles

**After treatment with GO**

There was no evidence of membrane damage; however, there was a high abundance of vacuoles in the examined cells. In some cells, intracellular accumulation of graphene was detected. In some hepatocytes, mitochondria were densely packed; however, in others the number of these organelles was decreased. Dark mitochondria with clearly visible cristae and dark matrixes were observed. Some hepatocytes had swollen mitochondria with poorly marked cristae. Mitochondrial leakings and the intramitochondrial inclusions were also noted (Fig. 3g, h).

**After treatment with rGO**

In some hepatocytes, a dismantled cytoplasm with decreased electron density and the signs of mitochondrial fragmentation were observed (Fig. 3c, d). There were a high number of cytoplasmic vacuoles in the vicinity of the damaged mitochondria. The rough endoplasmic reticulum around the mitochondria was distinctly observed. Dark mitochondria with the tendency to form branched and tubular structures were noted. The ratio of mitochondrial to cytoplasmic volume was lower compared to that of the control group. Swollen mitochondria with a disappearance of cristae were also noted.

**Concentration of 8-OHdG and TBARS in the liver**

The concentration of 8-OHdG was significantly decreased in the livers of embryos treated with pG and rGO at concentrations of 50 and 500 µg/ml compared to the control group and/or to the GO group (Table 3). TBARS were not affected by any of the treatments.

**Discussion**

The toxicity of three different graphene types including pG, GO, and rGO was evaluated. All types of graphene reduced the survival of chicken embryos to approximately 70–80 % for the high concentration (5000 µg/ml) while the survival was much lower for concentrations 50 and 500 µg/ml. Our previous results showed that pG administrated to the chicken embryos at levels from 50 to 10,000 µg/ml reduced chicken embryo survival, however, as in the present experiment, not in a dose-dependent manner. The reason for these results was the natural tendency of agglomeration of the pG flakes, compounded by proteins present in the embryo surroundings (Sawosz et al. 2014). It is hypothesized that the lower concentrations (50 and 500 µg/ml) of graphene penetrated the embryo more efficiently, comparing to the higher concentrations (5000 µg/ml) due to different nanoparticles dispersion level. Moreover, the differences between the different forms of graphene were also variable. The survival rate of embryos administered rGO was less than that of embryos administered either pG or GO. The observed differences may also be a consequence of the hydrophobic vs. hydrophilic character of the examined forms of graphene due to chemical groups available at the surface (Liao et al. 2011) and/or the size and shape of the graphene flakes (Akhavan et al. 2012). Moreover, according to Hu et al. (2011), nanomaterials can easily form “coronas” with proteins in biological systems, which also modify their toxicity.

Most of the studies conducted to date have not reported the animal death after administration of different forms of graphene (Duch et al. 2011; Yang et al. 2011). However, Wang et al. (2011) observed that GO administered intravenously under lower doses (0.1 and 0.25 mg) did not exhibit toxicity to mice, but at the dose of 0.4 mg 4 of 9 mice died. In the present study, we used a chicken embryo, which is a very sensitive and fast responding model. At the beginning of the embryogenesis the development of nervous and blood circulatory system takes place, making the embryo very sensitive to any external factors. Consequently, we suppose that the toxic effects of all types of graphene might be more potent during the early stages of rapid growth and development. Thus, we can speculate that the embryos, which survived this first period of life, could be less susceptible to graphene effects or were able to develop mechanisms of protection. At the later developmental stage, the body weight was only slightly reduced at the high dose (5000  $\mu\text{g/ml}$  of pG and rGO) but the weight of the examined organs (liver, heart, spleen, and brain) was not significantly affected by any type of graphene. Furthermore, the activities of ASP, ALT, and LDH (key blood markers of the liver destruction) did not differ, which is consistent with previous experiments with pristine graphene (Sawosz et al. 2014).

It has been demonstrated that graphene nanoparticles most commonly accumulate in the liver, spleen, and lungs (Wang et al. 2011; Yang et al. 2011; Zhang et al. 2011; Duch et al. 2011). Zhang et al. (2011) presented results from *in vivo* experiments that GO is cleared from the blood circulation within 48 h and accumulates primarily in the abovementioned organs. Recently, Yang et al. (2013a, b) confirmed that GO accumulates mainly in the liver and spleen after intraperitoneal injection; however, no inflammation was noted in these organs. On the contrary, an inflammatory response was observed by Wang et al. (2011) in mouse lungs and liver after GO intravenous administration. Zhang et al. (2011) observed no histopathological changes in the examined organs including the liver at a high GO dosage. The distinctive results presented by various authors may appear due to differences in the routes of administration, animal models, or nanographene preparations. Further studies are necessary to evaluate the effect of GO on animal organs.

To determine the impact of the different types of graphene on the liver with special emphasis on the potential localization of graphene in the liver, hepatocyte ultrastructure was analyzed with TEM. Morphological changes appeared within the hepatocyte cytoplasm and its organelles after treatment with all types of graphene. First of all, graphene accumulations were observed in the liver of the embryos in the GO group, which confirmed studies indicating that GO may accumulate within the cytoplasm or vacuoles of cells (Li et al. 2013). Jaworski et al. (2015) reported that GO and rGO have

different subcellular localizations in glioblastoma cells. The flakes of GO were located in both vacuoles and cytoplasm, while rGO was restricted to the cytoplasm. The localization may be affected by the hydrophilic/hydrophobic character of the graphene family. The rGO flakes are more hydrophobic in contrast to GO, which is recognized as a more hydrophilic form (Dreyer et al. 2010; Sanchez et al. 2012). Therefore, rGO is more likely to localize in vacuoles which are filled with water.

However, we observed the differences between the effects of pG, GO, and rGO on mitochondria. pG treatment caused not only swollen mitochondria but also damaged mitochondria with an interruption of the inner and outer membranes. Moreover, cristae were not clearly visible, sparse, or absent. In addition, the mitochondrial matrix was dense following pG treatment, and such high densities were not observed in the GO and rGO groups in which the matrix was lucent and the density was medium. The shape of the mitochondria were mainly oval in the pG-treated embryos, which differed from their shape in the GO and rGO groups and may indicate the involvement of some processes leading to mitochondrial fusion and fission and consequently to the stimulation of some repair processes. The present study is in line with previous results demonstrating effects on mitochondrial status. Depletion of mitochondrial membrane potential, ROS production, and apoptosis induced by graphene in macrophages has been observed (Li et al. 2012). The influence of graphene on the redox homeostasis interference and ROS production was suggested by additional studies (Zhang et al. 2010; Chang et al. 2011). Akhavan et al. (2012) confirmed that a concentration of 100  $\mu\text{g/ml}$  of rGO generates a high amount of ROS and elevated the percentage of DNA fragmentation and chromosomal aberrations. However, the effects observed in the present study cannot be directly compared with the above reports as they were carried out with *in vitro* models, but not with the intact organisms. Highly organized organisms may interact with nanomaterials differently than isolated cells or tissues via cooperation in-between the cells, tissues, and organs. Moreover, the environment within the body may interact with chemical groups exposed at the surface of graphene and modify the state of graphene, including agglomeration (Sawosz et al. 2014).

To assess the toxicity of graphene via oxidative stress mechanisms *in vivo*, two basic markers 8-OHdG and TBARS were measured (Kadiiska et al. 2005). 8-OHdG is a metabolite of DNA damage, while TBARS measurements correspond to malondialdehyde (MDA) levels. MDA is the main low-molecular-weight end product of the decomposition of certain primary and secondary lipid peroxidation products (Janero 1990). Interestingly, the 8-

OHdG levels were reduced in the pG and rGO groups, but not the GO group. As the level of 8-OHdG is proportional to DNA damage (Singh et al. 2011), the presented data suggest that pG and rGO may protect DNA from the damaging processes. Moreover, lipid peroxidation measured as TBARS concentration was not affected by the treatments. The key difference between DNA and lipid peroxidation is that molecules of DNA are protected against free radicals very efficiently and mainly highly reactive hydroxyl radicals (OH $\cdot$ ) that are produced via Fenton reactions are able to oxidize guanine, which is the most easily oxidized base in DNA (Sies 1997; Kobayashi and Tagawa 2003).

Qiu et al. (2014) demonstrated the antioxidant properties of graphene family materials toward OH $\cdot$  radicals in vitro, moreover, in the following order: few layers graphene (FLG) > rGO > GO. Our in vivo experiments confirmed this result, because rGO and pG showed significant properties of DNA oxidizing protection, while the effect of GO was probably very weak and not visible. We also agree that the mechanism of the activity may be the scavenging of reactive species such as OH $\cdot$ , the main detrimental radical for DNA, and also the observed mechanism may be associated with pristine sp<sup>2</sup> carbon domains, distinctive for pG and rGO (Qiu et al. 2014). Nevertheless, further investigation is required with a focus on graphene as a modulator of redox homeostasis examined in vivo.

The observed antioxidant property of pG and rGO indicates that the toxic effect induced by graphene in the embryo model may not proceed via redox signaling.

## Conclusion

The present studies indicated harmful effects of graphene family materials on chicken embryos, but only when applied at high doses. The harmful effects were observed as ultrastructural changes of the liver, including vacuolization and mitochondrial disruption. The observed changes differed in details and were specific for different forms of graphene. Moreover, pG and rGO treatments were associated with reduced levels of 8-OHdG in the chicken embryo liver. This data suggests that graphene administered in properly established doses may not exert toxic effect on the treated organism. Further in vivo studies with different animal models are necessary to clarify the level of toxicity of different types of graphene and to estimate the concentrations appropriate to evaluate their biomedical applications and environmental hazard.

**Acknowledgments** This work is part of the first author's habilitation thesis, and it was supported by the Polish National Research Council grant NCN OPUS 2011/03/B/NZ9/03387.

## Compliance with ethical standards

**Conflict of interest** The authors declare that they have no conflict of interest.

## References

- Akhavan O, Ghaderi E, Akhavan A (2012) Size-dependent genotoxicity of graphene nanoplatelets in human stem cells. *Biomaterials* 33: 8017–8025
- Bianco A (2013) Graphene: safe or toxic? The two faces of the medal. *Angew Chem Int Ed Eng* 52:4986–4997
- Chang Y, Yang S-T, Liu JH, Dong E, Wang Y, Cao A, Liu Y, Wang H (2011) In vitro toxicity evaluation of graphene oxide on A549 cells. *Toxicol Lett* 200:201–210
- Chen GY, Yang HJ, Lu CH, Chao YC, Hwang SM, Chen CL, Lo KW, Sung LY, Luo WY, Tuan HY, Hu YC (2012) Simultaneous induction of autophagy and toll-like receptor signaling pathway by graphene oxide. *Biomaterials* 33:6559–6569
- Chen Y, Qi Y, Liu B (2013) Polyacrylic acid functionalized nanographene as a nanocarrier for loading and controlled release of doxorubicin hydrochloride. *J Nanomater* 1:1–8
- Chowdhury SM, Lalwani G, Zhang K, Yang JY, Neville K, Sitharaman B (2013) Cell specific cytotoxicity and uptake of graphene nanoribbons. *Biomaterials* 34:283–293
- Dreyer DR, Park S, Bielawski CW, Ruoff RS (2010) The chemistry of graphene oxide. *Chem Soc Rev* 39(1):228–240
- Duch MC, Budinger GRS, Liang YT, Soberanes S, Urich D, Chiarella SE, Campochiaro LA, Gonzalez A, Chandel NS, Hersam MC, Mutlu GM (2011) Minimizing oxidation and stable nanoscale dispersion improves the biocompatibility of graphene in the lung. *Nano Lett* 11:5201–5207
- Fraga CF, Leibovitz BE, Tappel AL (1988) Lipid peroxidation measured as thiobarbituric acid-reactive substances in tissue slides. *Free Radic Biol Med* 4:155–161
- Gagnon ZE, Patel A (2007) Induction of metallothionein in chick embryos as a mechanism of tolerance to platinum group metal exposure. *J Environ Sci Health A Toxicol Hazard Subst Environ Eng* 42(3):381–387
- Geim AK, Novoselov KS (2007) The rise of graphene. *Nat Mater* 6(3): 183–191
- Hamburger V, Hamilton HL (1952) A series of normal stages in the development of the chick embryo. *Dev Dyn* 95:231–272
- Hinzmann M, Jaworski S, Kutwin M, Jagiełło J, Koziński R, Wierzbicki M, Grodzik M, Lipińska L, Sawosz E, Chwalibog A (2014) Nanoparticles containing allotropes of carbon have genotoxic effects on glioblastoma multiforme cells. *Int J Nanomedicine* 9:2409
- Hu W, Peng C, Lv M, Li X, Zhang Y, Chen N, Fan C, Huang Q (2011) Protein corona-mediated mitigation of cytotoxicity of graphene oxide. *ACS Nano* 5(5):3693–3700
- Janero DR (1990) Malondialdehyde and thiobarbituric acid-reactivity as diagnostic indices of lipid peroxidation and peroxidative tissue injury. *Free Radic Biol Med* 9(6):515–514
- Jastrzębska AM, Kurtycz P, Olszyna AR (2012) Recent advances in graphene family materials toxicity investigations. *J Nanopart Res* 14(12):1320–1328
- Jaworski S, Sawosz E, Kutwin M, Wierzbicki M, Hinzmann M, Grodzik M, Winnicka A, Lipińska L, Włodyga K, Chwalibog A (2015) In vitro and in vivo effects of graphene oxide and reduced graphene oxide on glioblastoma. *Int J Nanomedicine* 10:1585–1596
- Kadiiska MB, Gladen BC, Baird DD, Graham LB, Parker CE, Ames BN, Basu S, Fitzgerald GA, Lawson JA, Marnett LJ, Morrow JD,



- Murray DM, Plastaras J, Roberts LJ, Rokach J, Shigenaga MK, Sun J, Walter PB, Tomer KB, Barrett JC, Mason RP (2005) Biomarkers of oxidative stress study II: are oxidation products of lipids, proteins, and DNA markers of CCl<sub>4</sub> poisoning? *Free Radic Biol Med* 38: 698–710
- Kobayashi K, Tagawa S (2003) Direct observation of guanyl radical cation deprotonation in duplex DNA using pulse radiolysis. *J Am Chem Soc* 125:10213–10218
- Kurantowicz N, Sawosz E, Jaworski S, Kutwin M, Strojny B, Wierzbiński M, Szeliga J, Hotowy A, Lipińska L, Kozinski R, Jagiełło J, Chwalibog A (2015) Interaction of graphene family materials with *Listeria monocytogenes* and *Salmonella enterica*. *Nanoscale Res Lett* 10:23
- Lanphere JD, Rogers B, Luth C, Bolser CH, Walker S (2014) Stability and transport of graphene oxide nanoparticles in groundwater and surface water. *Environ Eng Sci* 31(7):350–359
- Li B, Yang J, Huang Q, Zhang Y, Peng C, Zhang Y, He H, Shi J, Li W, Hu J, Fan C (2013) Biodistribution and pulmonary toxicity of intratracheally instilled graphene oxide in mice. *NPG Asia Mater* 5. doi:10.1038/am.2013.7
- Li Y, Liu Y, Fu Y, Wei T, Le Guyader L, Gao G, Liu RS, Chang YZ, Chen C (2012) The triggering of apoptosis in macrophages by pristine graphene through the MAPK and TGF- $\beta$  signaling pathways. *Biomaterials* 33:402–411
- Liao KH, Lin YS, Macosko CW, Haynes CL (2011) Cytotoxicity of graphene oxide and graphene in human erythrocytes and skin fibroblasts. *ACS Appl Mater Interfaces* 3:2607–2615
- Liu J, Cui L, Losic D (2013) Graphene and graphene oxide as new nanocarriers for drug delivery applications. *Acta Biomater* 9(12): 9243–9257
- Qiu Y, Wang Z, Owens AC, Kulaots I, Chen Y, Kane AB, Hurt RH (2014) Antioxidant chemistry of graphene-based materials and its role in oxidation protection technology. *Nanoscale* 6(20):11744–11755
- Sanchez VC, Jachak A, Hurt RH, Kane AB (2012) Biological interactions of graphene-family nanomaterials: an interdisciplinary review. *Chem Res* 25(1):15–34
- Sawosz E, Jaworski S, Kutwin M, Hotowy A, Wierzbiński M, Grodzik M, Kurantowicz N, Strojny B, Lipińska L, Chwalibog A (2014) Toxicity of pristine graphene in experiments in a chicken embryo model. *Int J Nanomedicine* 9:3913–3922
- Sies H (1997) Oxidative stress: oxidants and antioxidants. *Exp Physiol* 82:291–295
- Singh SK, Szulik MW, Ganguly M, Khutsishvili I, Stone MP, Marky LA, Gold B (2011) Characterisation of DNA with an 8-oxoguanine modification. *Nucleic Acids Res* 39:6789–6801
- Vallabani NV, Mittal S, Shukla RK, Pandey SR, Dhakate SR, Pasricha R, Dhawan A (2011) Toxicity of graphene in normal human lung cells (BEAS-2B). *J Biomed Nanotechnol* 7(1):106–107
- Wang K, Ruan J, Song H, Zhang J, Wo Y, Guo S, Cui D (2011) Biocompatibility of graphene. *Nanoscale Res Lett* 6:8
- Yang K, Gong H, Shi X, Wan J, Zhang Y, Liu Z (2013a) In vivo biodistribution and toxicology of functionalized nano-graphene oxide in mice after oral and intraperitoneal administration. *Biomaterials* 34:2787–2795
- Yang K, Li Y, Tan X, Peng R, Liu Z (2013b) Behavior and toxicity of graphene and its functionalized derivatives in biological systems. *Nanotoxicology* 9:1492–1503
- Yang K, Wan J, Zhang S, Zhang Y, Lee ST, Liu Z (2011) In vivo pharmacokinetics, long-term biodistribution, and toxicology of PEGylated graphene in mice. *ACS Nano* 5:516–522
- Zhang X, Hu W, Jing Li J, Tao L, Wei Y (2012) A comparative study of cellular uptake and cytotoxicity of multi-walled carbon nanotubes, graphene oxide, and nanodiamond. *Toxicol Res* 1:62–68
- Zhang X, Yin J, Peng C, Hu W, Zhu Z, Li W, Fan C, Huang Q (2011) Distribution and biocompatibility studies of graphene oxide in mice after intravenous administration. *Carbon* 49: 986–995
- Zhang Y, Ali SF, Dervishi E, Xu Y, Li Z, Casciano D, Biris AS (2010) Cytotoxicity effects of graphene and single-wall carbon nanotubes in neural pheochromocytoma-derived PC12 cells. *ACS Nano* 4: 3181–3186